Earth's Future

RESEARCH ARTICLE
10.1029/2021EF002061

Economic Shock in a Climate Scenario and Its Impact on Surface Temperatures

Qi Ran[1,2], Shao-Yi Lee[1,2], John C. Moore[3,4,5], Chao Min[1], and Wenjie Dong[1,2]

[1]School of Atmospheric Sciences, Key Laboratory of Tropical Atmosphere-Ocean System, Ministry of Education, Sun Yat-sen University, Zhuhai, China, [2]Southern Marine Science and Engineering Guangdong Laboratory (Zhuhai), Zhuhai, China, [3]College of Global Change and Earth System Science, Beijing Normal University, Beijing, China, [4]Arctic Centre, University of Lapland, Rovaniemi, Finland, [5]CAS Center for Excellence in Tibetan Plateau Earth Sciences, Beijing, China

Key Points:

- Simulations of the climate response to three idealized scenarios reflecting a global economic crisis caused by a two-year home quarantine
- Substantial reductions in carbon dioxide and aerosol emissions resulted in short-term warming, followed by cooling until the end of simulation
- Greatest warming occurred over Europe in response to reductions in aerosols and persisted for two decades, which was explained by North Atlantic Oscillation phase

Supporting Information:

Supporting Information may be found in the online version of this article.

Correspondence to:

W. Dong,
dongwj3@mail.sysu.edu.cn

Citation:

Ran, Q., Lee, S.-Y., Moore, J. C., Min, C., & Dong, W. (2021). Economic shock in a climate scenario and its impact on surface temperatures. *Earth's Future*, *9*, e2021EF002061. https://doi.org/10.1029/2021EF002061

Received 12 MAR 2021
Accepted 27 MAY 2021

Author Contributions:

Conceptualization: Shao-Yi Lee, Wenjie Dong
Data curation: Qi Ran
Formal analysis: Qi Ran, Shao-Yi Lee
Methodology: Qi Ran, Shao-Yi Lee, Chao Min
Project Administration: Wenjie Dong
Software: Qi Ran
Visualization: Qi Ran
Writing – original draft: Qi Ran, Shao-Yi Lee
Writing – review & editing: Qi Ran, Shao-Yi Lee, John C. Moore

Abstract A socio-economic crisis was added to the Intergovernmental Panel on Climate Change (IPCC) Representative Concentration Pathway 8.5 (RCP8.5) scenario. This idealized climate scenario was simulated using the Community Earth System Model version 1.2.2 to determine the transient climate response to a two-year reduction of anthropogenic emissions. Global and regional (Asian, North American and European) mean surface temperatures (MSTs) were significantly warmer than baseline for 5 years. This was followed by cooler-than-baseline MSTs lasting for about two decades until the end of the simulation. Emission reduction of only carbon dioxide (CO_2) resulted in multi-decadal cooler-than-baseline MSTs. Emission reduction of aerosols and aerosol precursors resulted in strong short-term warmer-than-baseline MSTs for the first five years after the start of the crisis. This was followed by weaker multi-decadal warmer-than-baseline MSTs. The greatest warming occurred over Europe. This could be explained by the inter-scenario differences in the state of the North Atlantic Oscillation. However, global, Asian and North American MSTs were all warmer than baseline.

Plain Language Summary An Earth System Model was used to examine the climate impact of hypothetical two-year emission reductions due to a socio-economic crisis. Global and regional (Asian, North American and European) mean surface temperatures warmed immediately compared to the baseline scenario and continued for five years. This was followed by a cooling that lasted for decades. Emission reduction of only carbon dioxide resulted in multi-decadal cooling. Emission reduction of only aerosols resulted in strong short-term warming followed by weaker multi-decadal warming.

1. Introduction

With the exception of volcanic eruptions, rapid emission changes of greenhouse gases or aerosols in nature are more hypothetical than realistic. "Rapid" in this study refers to the human sense of a few years, rather than "rapid" in the geological sense of centuries which has occurred naturally in paleo-history (Bowen et al., 2015). Transient climate responses to such rapid emission changes in nature have been extensively studied (e.g., Bethke et al., 2017; Raible et al., 2016). The climate responses to hypothetical rapid changes or reversals of anthropogenic emissions have also been extensively studied (Bryan et al., 1982; Gregory & Webb, 2008; Held et al., 2010). Some studies examined transient responses lasting a year or two (Lohmann et al., 2010; Sherwood et al., 2015), while others examine more persistent responses over centuries to solar radiation management geo-engineering, such as stratospheric aerosol injection inspired by the former (Irvine et al., 2019; Schmidt et al., 2012).

Are rapid changes of anthropogenic emissions possible, however? Since these emissions depend on human activities, one might expect rapid declines during severe socio-economic crises. Accordingly, some form of transient climate response is possible in reality as well. The atmospheric lifetimes of anthropogenic greenhouse gases such as carbon dioxide and methane are measured in decades, but anthropogenic aerosols have shorter atmospheric lifetimes. Anthropogenic aerosols have been estimated to offset one-third of global warming driven by greenhouse gases since the 1950s (IPCC, 2013), although their temperature effects are spatio-temporally heterogeneous due to their shorter lifetimes (Persad & Caldeira, 2018; Wang et al., 2016). Hence, a transient climate response to emission reductions from socio-economic crises might have the form

of a slower response to greenhouse gas changes, and a faster response to aerosol changes, although the total response is not expected to be a linear sum of the two individual components.

Rapid changes of anthropogenic emissions have now been confirmed instrumentally. The existence of a novel coronavirus was first confirmed in Wuhan, China in December 2019. On March 11, 2020, the World Health Organization declared the now-named COVID-19 outbreak a pandemic. As many countries implemented partial or complete lockdowns to control the spread of the virus, there have been reported drops in the emissions of air pollutants (Copernicus Atmosphere Monitoring Service, 2020; European Space Agency, 2020a, 2020b, 2020c, 2020d, 2020e; Sharma et al., 2020; Volcovici, 2020), as well as carbon dioxide (Evans, 2020; Z. Liu et al., 2020; Papale et al., 2020).

The reality of such emission drops motivated this study, which simulated climate responses to a stylized 2-year pandemic-driven economic crisis. While one would expect in theory short-term warming in regions with the highest anthropogenic aerosol emissions, it is doubtful whether a transient reduction in greenhouse gas emissions would have a detectable signal amidst internal multi-decadal climate variability and long-term warming from past emissions (Solomon et al., 2010). It is furthermore doubtful if the short-term signal from aerosol emission changes can be detected amidst internal inter-annual climate variability. For detection purposes, exaggerated changes to the emissions were introduced to produce an envelope of the most extreme climate responses. This is not a study of the precise climate effects of COVID-19. Instead, this study examines if there could be a transient climate response to an economic crisis, and if so, what the transient climate response to an economic crisis would look like.

2. Methods

Three sensitivity experiments were created based on the Representative Concentration Pathway 8.5 scenario (RCP8.5). The RCP8.5 scenario was created for the fifth Climate Model Intercomparison Project (CMIP5) (Taylor et al., 2012), as a high emission scenario leading to 8.5 Wm^{-2} increase in radiative forcing by the end of the century (Moss et al., 2010; Riahi et al., 2007). While slated to be replaced by a combination of RCPs and the new Shared Socioeconomic Pathways (SSPs) in the CMIP6 (Eyring et al., 2016; Gidden et al., 2019), the RCP8.5 climate projections have been more widely studied than the more recent CMIP6. Emissions do not vary much between RCP scenarios before 2020 (Figure S1.1 and IPCC, 2014), but thereafter increase the most in RCP8.5; RCP8.5 is considered the most pessimistic climate scenario for the 21st century.

The sensitivity experiments were highly idealized and designed to test the upper and lower bounds on the model response, rather than precisely track the complex spatiotemporal changes of an actual crisis, such as studies like Le Quéré et al. (2020). The first experiment (ALL) assumes that travel and industrial activities have been completely halted, such that anthropogenic air pollutant emissions in these sectors are zero. At the same time, carbon dioxide concentrations are held constant for the duration of the crisis. Anthropogenic carbon dioxide and air pollutant emissions are linked, but for simplicity natural carbon dioxide sinks were assumed to have increased to equilibrate with the lower emissions, for example, through recovery of land and ocean ecologies, resulting in no further increase. The crisis was assumed to last for 2 years. The second and third experiments limit the changes to air pollutants alone (AER), and carbon dioxide alone (CO2). More information on the experiment design is provided in Section 2.2.

2.1. Model

The simulations were conducted using the Community Earth System Model (CESM) version 1.2.2 (Hurrell et al., 2013). The baseline experiment was the B_RCP8.5_CAM5_CN component set, a fully coupled configuration including the Community Atmosphere Model 5 (CAM5; Neale et al., 2010), Parallel Ocean Program version 2 (POP2), Community Land Surface Model (CLM) version 4.0, the Los Alamos sea ice model (CICE) version 4, all coupled together using the CESM coupler CPL7. The horizontal resolution of CAM5 and CLM was 1.9° × 2.5° latitude-longitude (f19 grid), while that of POP2 and CICE was about 1° (g1v6 grid). The vertical coordinate of CAM5 was a hybrid sigma-pressure system consisting of 30 vertical levels, with model top at about 3.6 hPa. CLM had 15 soil layers to 35 m depth, POP2 had 60 height layers, and CICE had five thickness categories. These are the default configuration of the B_RCP8.5_CAM5_CN configuration.

The simulations were run with the Modal Aerosol Module with three modes (MAM3). Since the concentrations produced by the more sophisticated seven mode version (MAM7) were found to be generally well reproduced by MAM3 (X. Liu et al., 2012), the default option of the RCP8.5 scenario was retained. Emissions were based on AeroCom (Aerosol Comparisons between Observations and Models; Textor et al., 2005), but ammonia was prognostic in the simplified chemistry of MAM3. Anthropogenic primary black carbon, primary organic matter, sulfur dioxide and sulfates were emitted in seven sectors—agriculture, waste, domestic, energy, industrial, transportation, shipping.

2.2. Experiment Design

An ensemble of simulations is the standard approach for extracting the response to forcing from natural climate variability (Kay et al., 2015; C. Li et al., 2020; Smith et al., 2019). Larger ensembles are desirable but incur additional computational costs. Studies indicate that at least 10 ensemble members are necessary for robust conclusions (Bittner et al., 2016; Hermanson et al., 2020; Swingedouw et al., 2017). Hence, 10-member ensembles were used in this study. Each member of a scenario was subjected to the same radiative forcing scenario, but begun from a slightly different initial atmospheric state on January 1, 2005. The initial state was created by randomly perturbing temperatures using different round-off errors (Kay et al., 2015).

The baseline scenario was the default RCP8.5. CO_2 concentrations and aerosol-related emissions of the three sensitivity experiments followed RCP8.5 until 2020, then followed the values of their specific scenarios until 2050, as detailed below.

Under the quarantine scenario, emissions in the industrial, transportation and shipping sectors were assumed to be affected. Emissions in the agricultural, waste, domestic, and energy sectors were assumed to be unchanged. In the scenario denoted by "AER", aerosol and aerosol precursor emissions in the affected sectors were set to zero for 2 years from 2020 to 2021. Precursor gases in the toluene, big alkane, and big alkene categories were considered anthropogenic and set to zero in the crisis scenario. Isoprene and monoterpenes were considered natural and unchanged. Biomass burning, volcanic, and ocean emissions were unchanged. The spatial patterns of emissions before and after reduction are shown in Figure 1. The largest emission reduction of all the aerosols and aerosol-precursors was over Asia.

In the scenario denoted by "CO2", carbon dioxide concentration followed RCP8.5 until December 2019, was set to remain constant in the crisis for 2 years from January 2020 to December 2021, then resumed its upward trend from January 2022 as if it were 2020 in the default RCP8.5 scenario (Figure S1.2). Other well-mixed greenhouse gases (CH_4, N_2O and halocarbons) continued to follow the RCP8.5 scenario. CH_4 and N_2O were more agricultural than industrial emissions, and agricultural production was assumed to be unchanged in the scenario.

In the scenario denoted by "ALL", carbon dioxide concentrations followed the CO2 scenario, while aerosols and aerosol precursors followed the AER scenario.

Additional technical details on the implementation of the two-year event are summarized in Table 1. Aerosol and precursor emissions in the default MAM3 input were provided only once every 10 years, while CO_2 concentrations were provided for the July of every year. To simulate the two-year event, the baseline was started from 2005 using the provided restart file, integrated to 2020, then halted. Three branches were created from the baseline (AER, CO2, ALL), then integrated for two more years with altered forcing. The three branches were halted after 2 years of simulation, then restarted with recovered emissions of air pollutants under RCP8.5 (AER, ALL) and time-shifted carbon dioxide concentrations (CO2, ALL). All scenarios were simulated to 2050. The RCP8.5 scenario was simulated from 2020 to 2050 without any changes.

2.3. Post-Processing

This study focuses on the mean surface temperature (MST) over the whole globe and three regions: Asia, Europe, North America (Figure 2a and 2b). The MST was area-weighted using the cosine of latitudes. For the decadal analysis, signals shorter than 7 years were removed with a Lanczos low-pass filter (Duchon et al., 1979). Supplementary Material S3 show the raw time series and their frequency spectra that were used to determine the 7-year filter threshold. Global and regional MST time series were filtered before ensemble

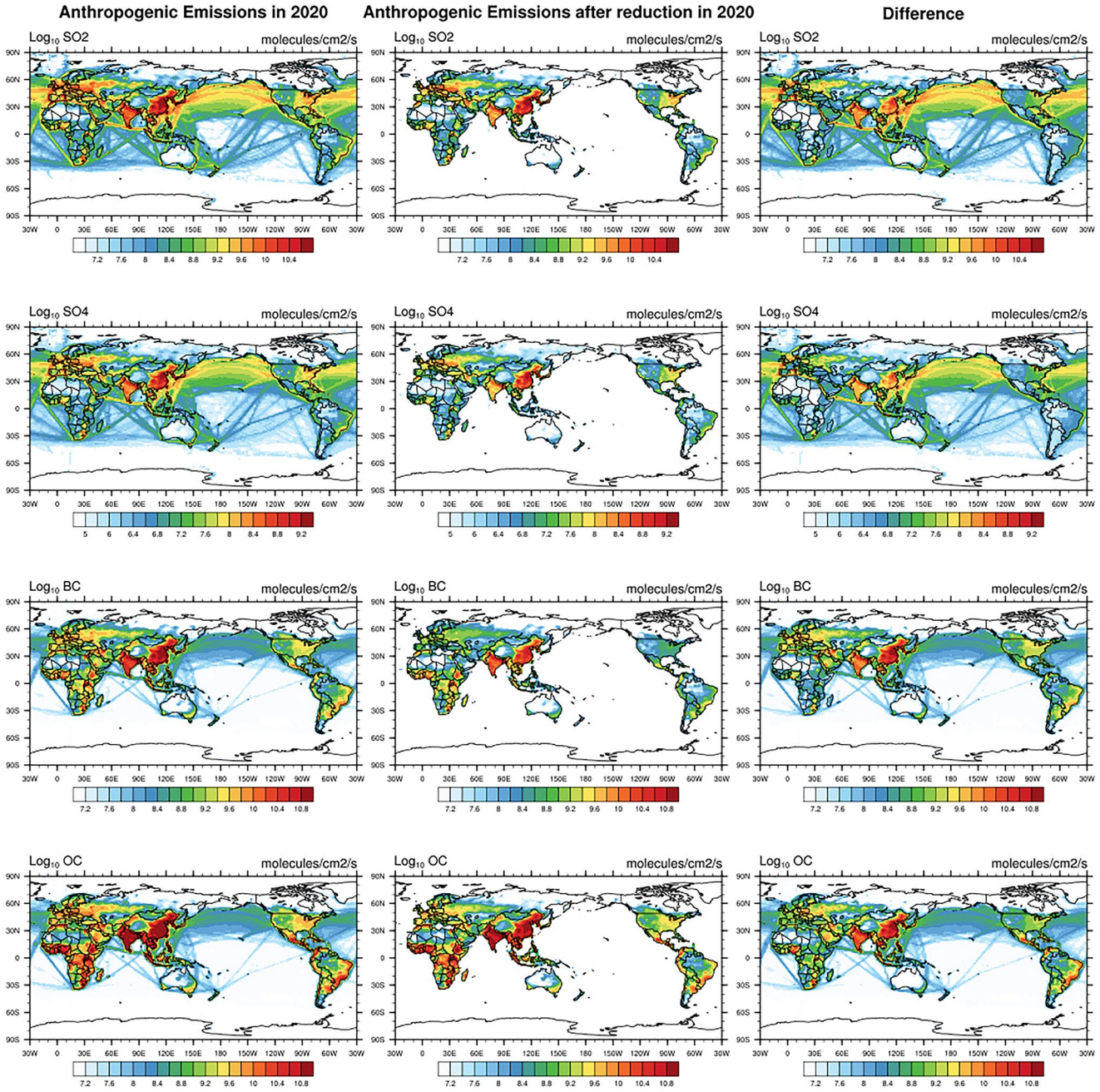

Figure 1. Annual mean air pollutant emissions (plotted by log of molecule cm^{-2} s^{-1} concentration) in 2020 in the Representative Concentration Pathway 8.5 scenario (left column), after reduction (middle column) and change after reduction (right column), for sulfur dioxide (SO_2; first row), sulphate (SO_4; second row), black carbon (BC; third row), Organic carbon (OC; fourth row). Secondary organic aerosol gases that were assumed to be anthropogenic (see text) were completely removed (so not shown here).

averaging. Differences between a sensitivity experiment and the baseline were calculated using the ensemble mean of filtered MST; the baseline result was subtracted from the perturbed results of the scenario in question. Taking the difference between two scenarios removes any shared biases or drifts in the simulated climate.

Statements about whether the perturbed climates were warmer or cooler than baseline climates were evaluated with the non-parametric Wilcoxon signed-rank test. The one-tailed test was carried out at 0.10, 0.05, and 0.025 significance levels. Significant levels of 0.10 and 0.05 are more commonly used and the 0.025

Table 1
Emission Scenarios of the Baseline Experiment and the Three simulations

Scenario	Simulated time	Aerosol emissions	CO_2 concentration
RCP8.5	01/2005–2012/2050 (MM/YYYY)	RCP8.5 scenario	RCP8.5 scenario
AER	01/2020–12/2021	ITS emissions set to zero	RCP8.5 scenario
	01/2022–12/2050	RCP8.5 scenario	
CO2	01/2020–12/2021	RCP8.5 scenario	Held at the concentration in January 2020 of RCP8.5
	01/2022–12/2050		Resumed its growth rate of RCP8.5 scenario (cf. Figure S1.2)
ALL	01/2020–12/2021	ITS emissions set to zero	Held at the concentration in January 2020 of RCP8.5
	01/2022–12/2050	RCP8.5 scenario	Resumed its growth rate of RCP8.5 scenario (cf. Figure S1.2)

Abbreviations: AER, reduced air pollutants only; ALL, reduced air pollutants and carbon dioxide; CO2, reduced carbon dioxide only; ITS, Industrial, Transportation and Shipping; RCP8.5, Representative Concentration Pathway 8.5.

value should be considered an extremely strict threshold. Individual years were tested, as well as the two periods of 2020–2025 and 2020–2050, described as "short-term" and "long-term", respectively. As a reference, the typically used *t*-test 80% confidence intervals were estimated every year for the MST and the North Atlantic Oscillation Index (NAOI), with the caveat that the underlying assumption (i.e., the 10 ensemble

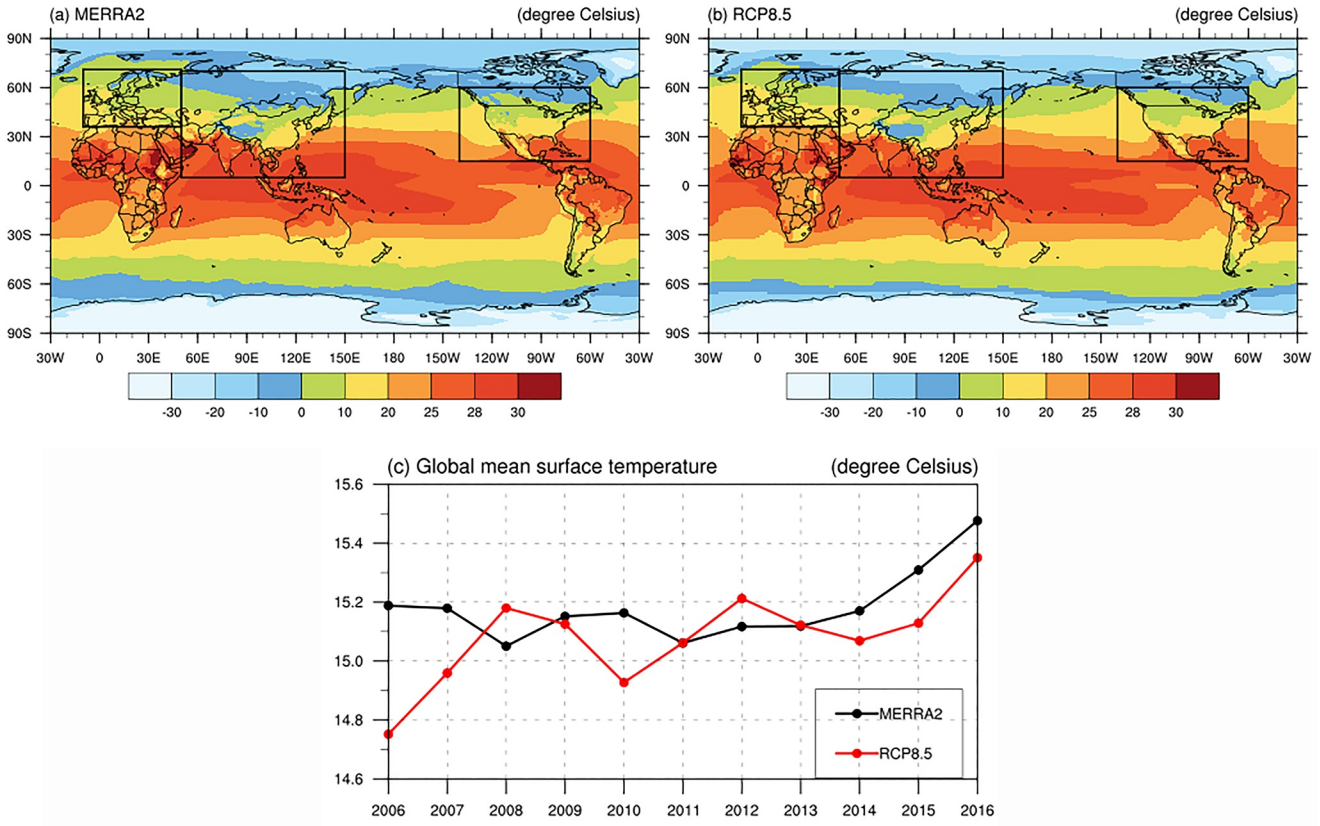

Figure 2. Multi-year average global surface temperatures over 2008–2012 for (a) Modern-Era Retrospective analysis for Research and Applications Version 2 (MERRA2) with horizontal resolution 0.5° × 0.625°, and (b) the Representative Concentration Pathway 8.5 (RCP8.5) simulation with horizontal resolution 1.9° × 2.5°. Black boxes in (a) and (b) represent the three analysis regions from left to right: Europe (36°N–71°N, 10°E–50°E); Asia (5°N–70°N, 50°E–150°E); North America (15°N–60°N, 140°W–160°W). (c) Global mean surface temperatures of MERRA and the RCP8.5 simulation.

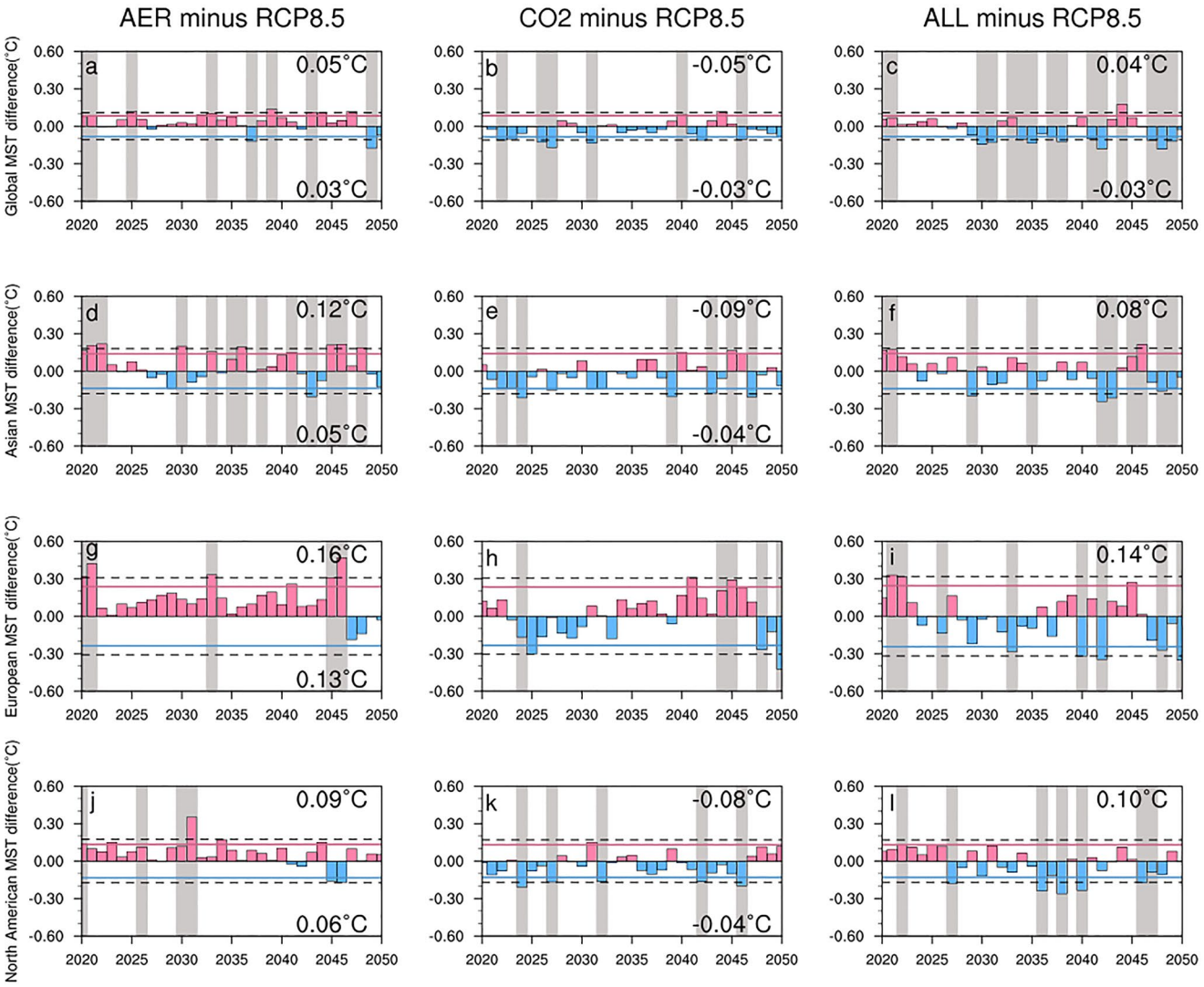

Figure 3. Ensemble mean unfiltered differences of annual mean surface temperature between the three sensitivity simulations and the Representative Concentration Pathway 8.5 (RCP8.5) baseline (columns, red bars indicate years warmer in scenarios than RCP8.5, blue bars cooler years), for the whole globe and three regions (rows). Gray shading marks periods when the differences were statistically significant under the one-tailed Wilcoxon signed rank test at 0.10 significance level, that is, the particular red (blue) year is significantly warmer (cooler) than baseline. Solid red (blue) lines demarcate the mean over 30 years (30 individual tests) threshold at which anomalies become significantly warmer (cooler) at 0.10 significance level, assuming Gaussian distributed anomalies (see Section 2.3). Dashed lines demarcate the mean threshold at 0.05 significance level. Numbers in the upper and lower left of each panel show the mean anomaly for the periods 2020–2025 and 2020–2050, respectively.

members being drawn from Gaussian distributions) may not be true. Anomaly plots (Figures 3 and 4) show the mean of these confidence intervals as red/blue horizontal lines, while magnitude plots (Figures 5 and 6) plot annual confidence intervals as shading.

The North Atlantic Oscillation Index (NAOI) used in this study was calculated thus: The mean surface pressure anomaly along 80°W to 30°E was calculated for 35°N and 65°N, normalized by standard deviation, and the difference taken. There is no singular methodology for calculating the NAOI, and this method of J. Li and Wang (2003) was selected for its ease of use. The standard deviation calculated from the period of 2005 to 2020 using values from all scenarios was used for normalization. The NAOI calculated using standard deviations from the 2005 to 2050 period of each simulation was qualitatively similar (not shown), and the shared standard deviation was used so that the NAOI from different scenarios were comparable. The NAOI for individual months was first calculated, then the December-January-February means was taken for analysis. Results using annual means were qualitatively similar (not shown), but the winter season mean was

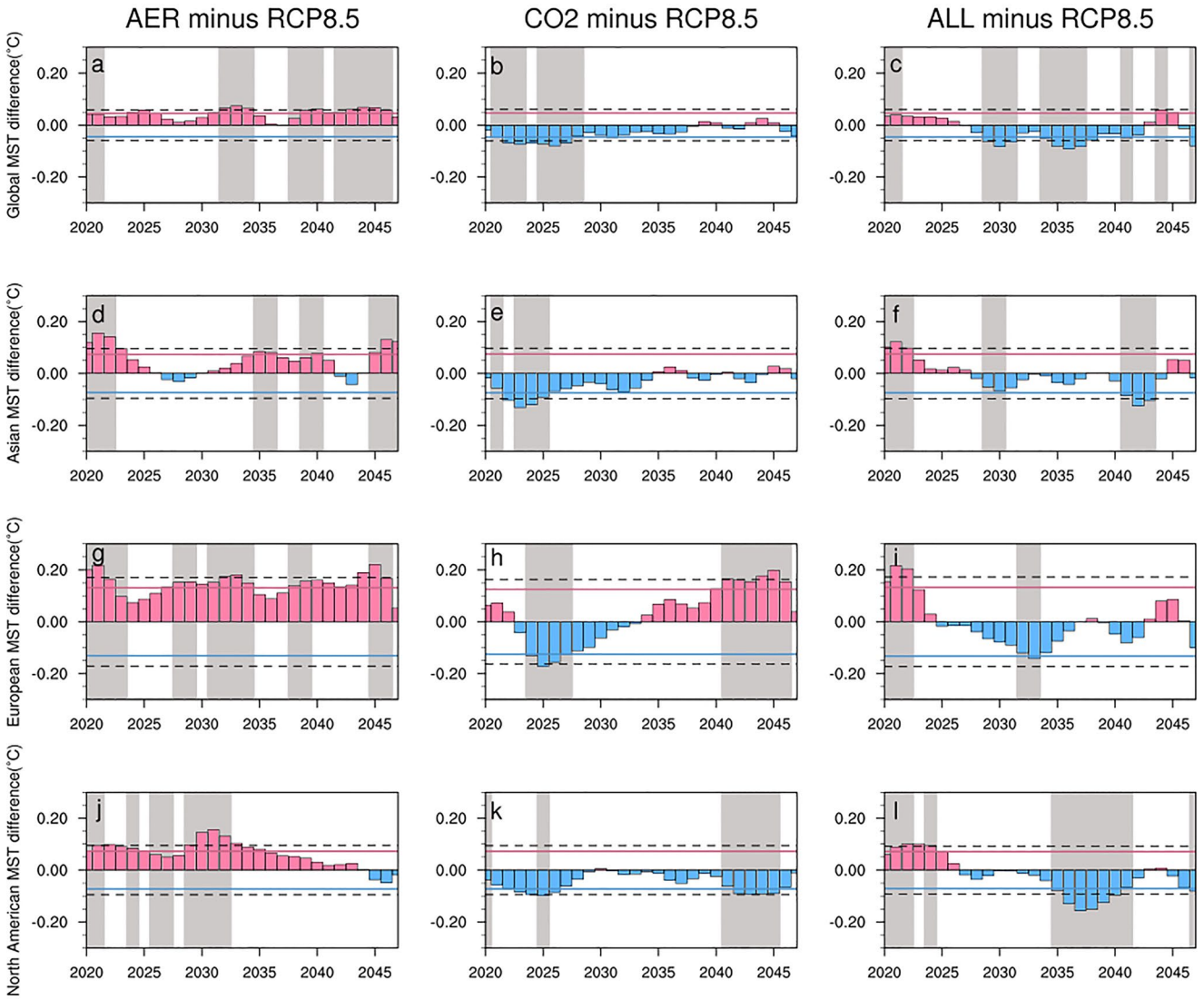

Figure 4. Similar to Figure 3 but the mean surface temperature of each simulation has been put through a 7-year low-pass Lanczos filter prior to the other treatments (see Section 2.3).

used to better reflect the winter season nature of the phenomenon. For decadal analysis, a 7-year Lanczos low-pass filter was applied before the ensemble mean was calculated.

3. Results

As shown in Figure 2, the spatial distribution of multi-year average surface temperature over 2008–2012 of the Modern-Era Retrospective analysis for Research and Applications Version 2 (MERRA2; Gelaro et al., 2017) was similar to that of the RCP8.5 simulation, as well as the trajectory of global MST. Surface temperature of the RCP8.5 simulation is that of the ensemble member whose initial atmospheric state was not perturbed. The period of 2008–2012 was selected based on panel Figure 2c, a period of relatively stable global MST for both datasets. Overall, the simulation satisfactorily reproduced historical surface temperatures, which provided confidence to estimate the trend of future surface temperatures under our hypotheses.

The differences between the three sensitivity simulations and the RCP8.5 baseline for ensemble mean unfiltered MST are shown in Figure 3. Figure 4 shows similar results for 7-year filtered MST, to give a sense of

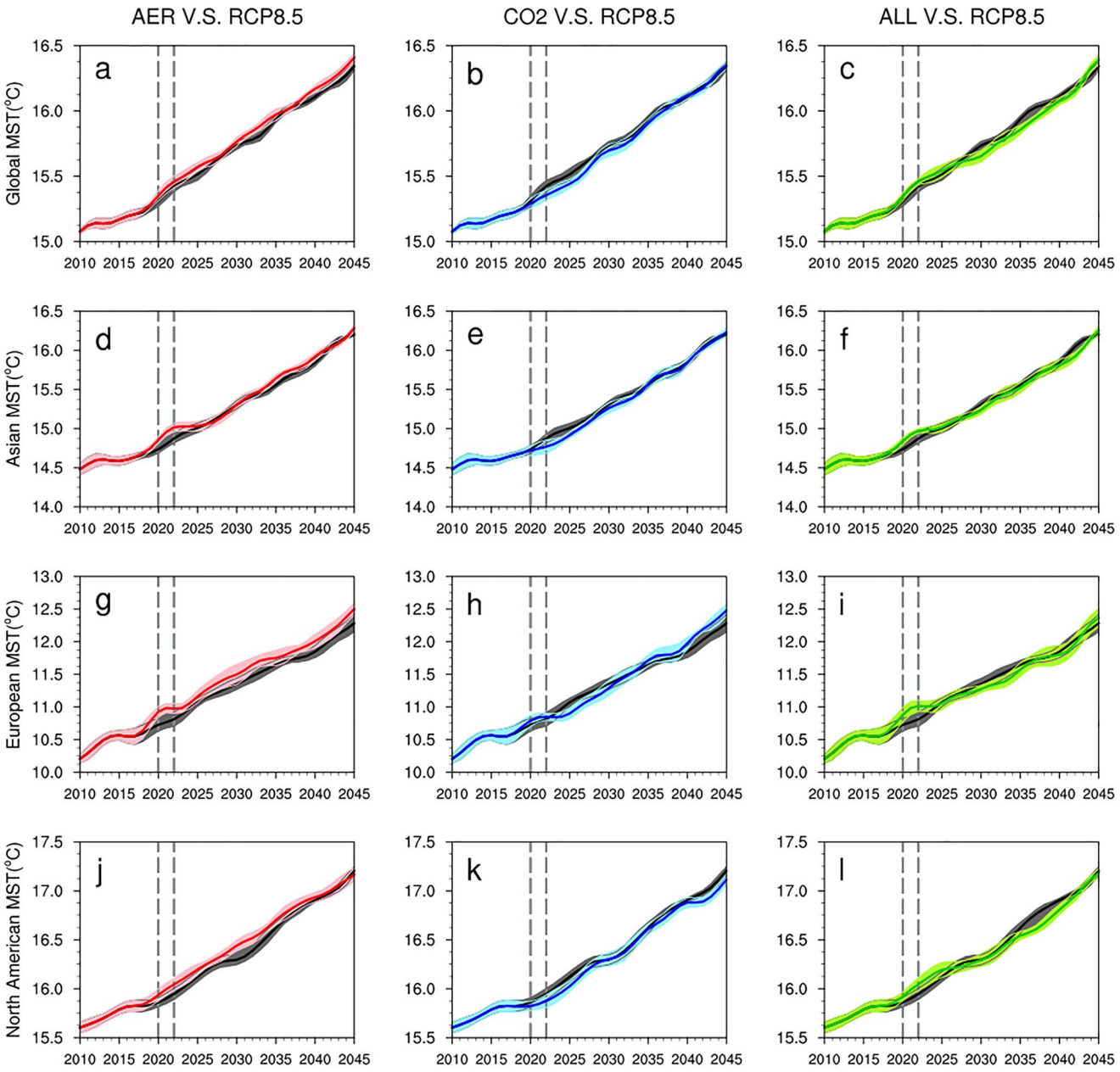

Figure 5. Comparison of ensemble mean filtered mean surface temperature from the three experiments with the baseline, over (a)–(c) the whole globe, (d)–(f) Asia, (g)–(i) Europe, (j)–(l) North America. Black solid line shows MST from Representative Concentration Pathway 8.5. Red solid line (left column): reduced air pollutants only (AER); Blue solid line (center column): reduced carbon dioxide only (CO2); Green solid line (right column): both reduced air pollutants and carbon dioxide (ALL). The shaded areas represent the 80% confidence interval. The gray dashed lines show the years in which emissions were reduced.

the differences in long term trends. Global means were calculated, as well as means over Asia, Europe, and North America (Figure 2a and 2b). Figure 5 shows the actual filtered MST trajectories; when the areas do not overlap, the perturbed experiment is significantly warmer or cooler using the one-tail Student's *t*-test at 0.10 significance level. Unfiltered curves are shown in Figure S3.1. The state of the Earth system at any particular labeled year only reflects the climatic state, and does not reproduce the phase of internal variability the real Earth lies in, even for the multi-decadal variability that remains after filtering.

10.1029/2021EF002061

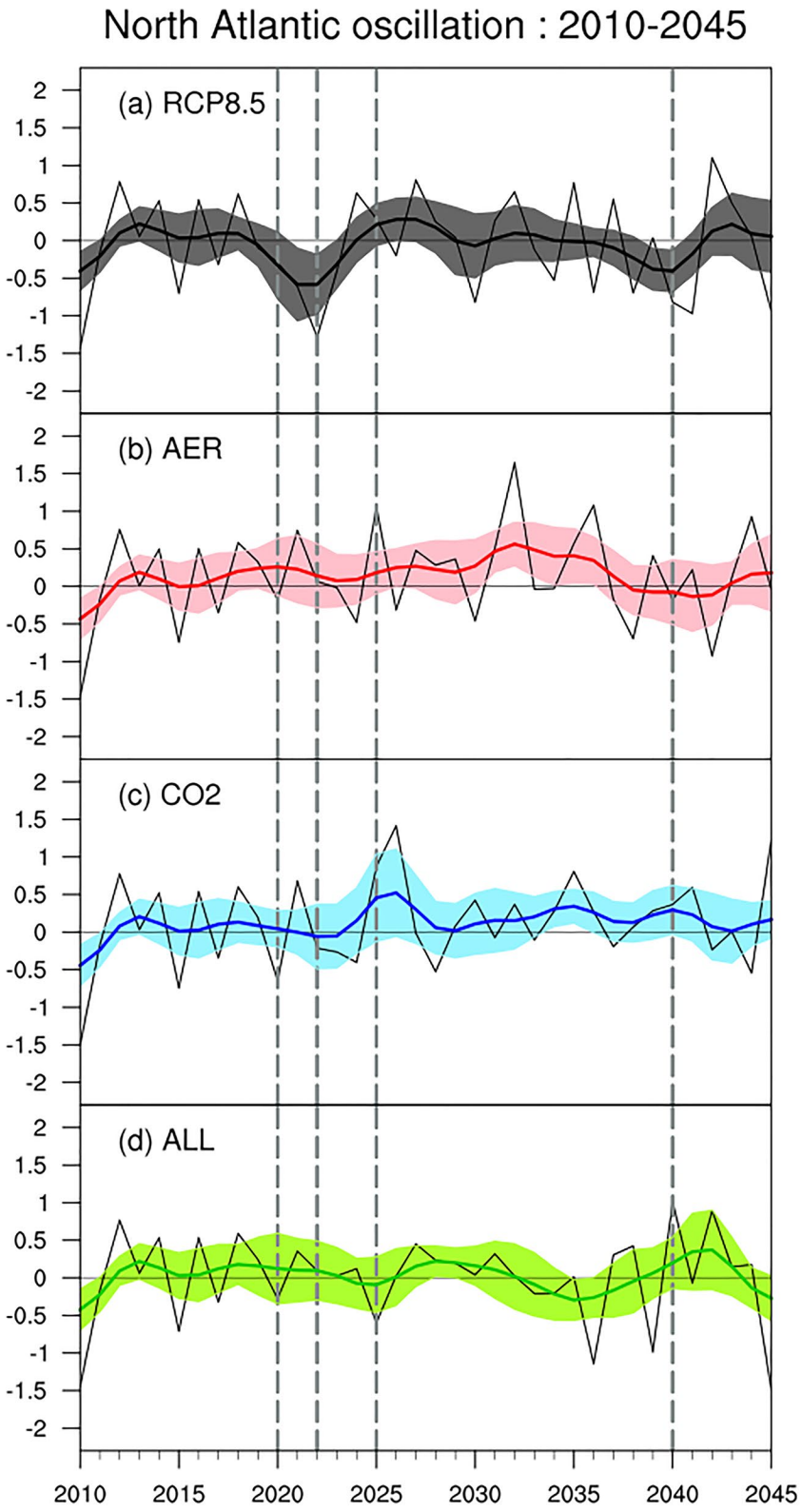

Figure 6. Ensemble mean normalized North Atlantic Oscillation Index of December-January-February from 2010 to 2045, for (a) Representative Concentration Pathway 8.5, (b) reduced pollutant only (AER), (c) reduced carbon dioxide only (CO2), (d) both reduced pollutant and carbon dioxide (ALL). Thin black lines show the unfiltered time-series. Thick colored lines show the NAOI time series that have been put through a 7-year low-pass filter prior to ensemble averaging. The vertical gray dash lines demarcate years 2020, 2022, 2025, and 2040. The shaded areas around the time series represent the 80% confidence intervals.

Table 2
Results of Statistical Testing for the Period of 2020–2025

Scenarios	Parameters		Global	Asia	Europe	North America
(a) AER versus RCP8.5	*p*-value		0.078	0.031	0.016	0.016
	α	0.100	Warmer	Warmer	warmer	warmer
		0.050				
		0.025				
(b) CO2 versus RCP8.5	*p*-value		0.016	0.047	0.422	0.031
	α	0.100	Cooler	Cooler		cooler
		0.050				
		0.025				
(c) ALL versus RCP8.5	*p*-value		0.016	0.078	0.078	0.016
	α	0.100	warmer	Warmer	warmer	warmer
		0.050				
		0.025				

Note. The Wilcoxon signed rank test was used to determine if the ensemble mean of unfiltered MST of this period was warmer/cooler in the sensitivity scenario compared to baseline (rows). The one-tailed test was carried out at three values of significance level α. The MST of the whole globe and three regions were tested (columns). When $p < \alpha$, the sensitivity scenario is significantly warmer/cooler as indicated in the table. When $p \geq \alpha$, results are not statistically significant as indicated by shaded cells.

Abbreviations: AER, reduced air pollutants only; ALL, reduced air pollutants and carbon dioxide; CO2, reduced carbon dioxide only; RCP8.5, Representative Concentration Pathway 8.5.

3.1. Changes in Mean Surface Temperature

As expected, the reduction in the emissions of aerosols and aerosol-precursors (scenario AER) resulted in significant immediate (years 2020–2021) warmer-than-baseline global MST (Figure 3a). Immediate warmer-than-baseline MSTs were seen in all of the three regions as well (Figures 3d, 3g, 3j). As shown in Table 2a, global and regional MSTs were significantly warmer than baseline in the short-term period, which we define as the 5 years including the start of the crisis (years 2020–2025). Uncertainty was greater for the global MST, as reflected in the larger *p*-value. Contrary to expectation that the impact on MSTs would only be immediate or short-term, warmer-than-baseline MSTs persisted for decades after the initial perturbation, both globally (Figure 4a) as well as over the three regions (Figures 4d, 4g, 4j). As shown in Table 3a, global and regional MSTs were significantly warmer than baseline in the long-term period, which we define as the 30 years including the start of the crisis (years 2020–2050).

When only carbon dioxide emission was reduced (scenario CO2), there was a lag time of about 2 years before any kind of cooling effect was seen in the global MST (Figure 3b). Cool anomalies compared to baseline dominated in the short-term and even until about 2035, though only sometimes significant. Regional MSTs reflect similar cooler-than-baseline patterns (Figures 3e, 3h, 3k). This cooling effect faded away after about 15 years (Figure 4b), perhaps becoming relatively unimportant compared with rising carbon dioxide concentrations (Figures 5b, 5e, 5h, 5k). From Tables 2b and 3b, global MST was significantly cooler than baseline in both the short-term and long-term. Asian and North American MSTs were significantly cooler as well, but not European MST.

The AER warming and CO2 cooling trends were visibly apparent in both the unfiltered (Figure 3 and Supplementary Figure S3.1, first and second columns) and filtered MSTs (Figures 4 and 5, first and second columns). The AER and CO2 scenarios map out two extremes, while a realistic scenario is expected to have weaker reductions in both air pollutants and carbon dioxide, resulting in a scenario intermediate between the two.

When both aerosol/aerosol precursors and carbon dioxide emissions were reduced (scenario ALL), significant immediate warming of the global MST occurred, by up to 0.06°C compared to the baseline (Figure 3c). Regional MSTs were also warmer than baseline (Figures 3f, 3i, 3l), particularly the European MST. From

Table 3
Similar to Table 2, but for the Period of 2020–2050

Scenarios	Parameters		Global	Asia	Europe	North America
(a) AER versus RCP8.5	*p*-value		0.002	0.028	4×10^{-5}	4×10^{-4}
	α	0.100	warmer	Warmer	warmer	warmer
		0.050				
		0.025				
(b)CO2 versus RCP8.5	*p*-value		0.004	0.032	0.373	0.025
	α	0.100	cooler	Cooler		cooler
		0.050				
		0.025				
(c)ALL versus RCP8.5	*p*-value		0.060	0.344	0.269	0.309
	α	0.100	cooler			
		0.050				
		0.025				

Abbreviations: AER, reduced air pollutants only; ALL, reduced air pollutants and carbon dioxide; CO2, reduced carbon dioxide only; RCP8.5, Representative Concentration Pathway 8.5.

Table 2c, global and regional MSTs were significantly warmer than baseline in the short-term period. The short-term warmer-than-baseline period was followed by a cooler-than-baseline trend until mid-century, with the maximum cooling of around 0.2°C (Figures 3c and 4c). From Table 3c, differences between perturbed and baseline MSTs were not statistically significant in the long-term. Global MST was significantly cooler at 0.10 significance level, with greater uncertainty as reflected in the larger *p*-value.

Comparison of ALL with the reduced aerosols/precursors only (AER) and the reduced carbon dioxide only (CO2) scenarios suggested the combined response of a short-term warming from reduced aerosols, followed by a long-term cooler-than-baseline trend caused by reduced carbon dioxide (Figures 4 and 5, third column). However, the changes in MSTs were not generally significant over the full duration of the experiment (Table 3c).

3.2. Comparison of Changes in Regional Mean Surface Temperatures

In short-term (2020–2025), the greatest warmer-than-baseline MST occurred over Europe in the AER scenario. This warmer-than-baseline European MST peaked in 2021, reaching about 0.4°C warmer unfiltered (Figure 3g) and about 0.2°C warmer filtered (Figure 4g). The MST was comparable to the baseline European MST in the late 2020s (Figure 5g). MSTs over all three regions were warmer than baseline in both ALL and AER scenarios, but the warming over North America was weaker compared to the other regions (Figures 3 and 4). This was consistent with the smallest absolute reduction in pollutant emissions over North America. Carbonaceous emissions-per-area reductions over Asia were 2.7 times larger than that over Europe, which in turn were 2.4 times that over North America; sulfur dioxide emissions-per-area reductions over Asia and Europe were double those over North America (Table S2). Correspondingly, Aerosol Optical Depth at 550 nm over all three regions showed short-term reductions from baseline in both ALL and AER scenarios, but the reduction over North America was almost half of the reductions over Asia or Europe (Figure S4). In summary, the greatest absolute reduction in aerosol/precursor emissions occurred over Asia, but the greatest warming from baseline occurred over Europe.

Atmospheric aerosol levels over Europe and North America returned to baseline levels by 2025 (Figure S4). Examining the filtered MST from the AER scenario, the significantly warmer-than-baseline European MST lasted for the duration of the simulation (Figures 4g and 5g). Filtered North American MST was warmer-than-baseline for about 2.5 decades after the crisis, until about 2045, or significantly warmer for about 1.5 decades until 2035 (Figures 4j and 5j). Asian MST was also warmer to a lesser extent (Figures 4d and 5d). Even in the CO2 scenario which was generally cooler than baseline, the filtered European MST was

significantly warmer than baseline after 2035 (Figures 4h and 5h), something not seen in the global, Asian or North American MSTs. In summary, atmospheric aerosol levels returned to baseline levels by around 2025, but their effect on global and regional MSTs appeared to persist for at least 10 years longer.

We address the two ambiguities raised above with a discussion of multi-decadal variability. An important consideration when analyzing perturbed climate experiments is the influence of natural modes of multi-decadal variability. These modes would ideally be removed with the use of ensembles, but perhaps not completely using a small ensemble. A major suspect for the multi-decadal discrepancies is the North Atlantic Oscillation (NAO), which is known to strongly affect the weather and climate in the North Atlantic basin and Western Europe. The negative phase of NAO is associated with cooling and the positive phase is related to warming over Europe (Kenyon & Hegerl, 2008; Pinto & Raible, 2012).

Figure 6 shows the NAOI in the four simulations. The ensemble mean unfiltered index (thin black line) is identical between simulations before 2020, then differs between simulations after 2020; the ensemble mean filtered indices (thick colored lines) give a better sense of the multi-decadal variability. For the baseline scenario, the NAO was strongly in the negative phase during 2020–2025, slightly positive for 2025–2030, and neutral-to-negative up to 2040 (Figure 6a). In contrast, the NAO was in the neutral phase during 2020–2025 for the three sensitivity scenarios (Figures 6b–6d). The inter-simulation phase of the NAO may influence the inter-simulation MST differences over Europe, and to some extent over North America. In the short-term period after the crisis (2020–2025), the baseline European MST would be cooler than typical due to its negative NAO phase.

The "cooler" CO2 scenario is discussed first, where European MST was found to be warmer than baseline during certain periods, against expectation. The neutral NAO phase (warmer-than-baseline multi-decadal variability) for the CO2 scenario would explain why European MST in the 2020–2025 period was not significantly different from baseline, even though global, Asian and North American MSTs were significantly cooler than baseline (Table 2b). A similar period was around 2040, where NAO for the baseline scenario was in the negative phase, but NAO for the three sensitivity scenarios was in the neutral phase. This would explain why European MST around 2040 was significantly warmer-than-baseline (Figure 4h). Due to these two warmer-than-baseline periods, European MST showed no statistically significant differences from baseline for the whole period of 2020–2050 (Table 3b).

The AER scenario is discussed next, where warmer-than-baseline MST anomalies persisted in the long-term, against expectation. As above-described, the NAO for the AER scenario was in the neutral phase during 2020–2025, compared to the negative phase for the baseline scenario. Furthermore, NAO for the AER scenario was in the positive phase during 2030–2035, compared to the neutral phase for the baseline scenario. Finally, the NAO for the AER scenario was in the neutral phase around 2040, but the NAO was in the negative phase for the baseline scenario. This would explain why European MST was warmer than baseline for most of 2020–2050.

The NAO phase seems unlikely to be responsible for all of the longer-lasting impacts. The above explanation might be justifiable for the persistently warmer-than-baseline North American MST, but the processing area covers most of North America including large areas of the Pacific Ocean. Asian and global MSTs were persistently warmer-than baseline as well. It is possible that other modes of multi-decadal variability may explain such temperature differences, such as the Pacific Decadal Oscillation (PDO) or the Arctic Oscillation (AO), but we do not wish to turn this study into a catalog of all possible climate variability modes.

4. Discussion and Conclusions

Since anthropogenic emissions depend on human activities, one might expect rapid declines during severe socio-economic crises. Accordingly, some form of transient climate response is possible in the wake of such crises. Such rapid declines in emission changes have now been confirmed instrumentally during the coronavirus pandemic of 2019, which is still ongoing at the time of writing. The Community Earth System Model version 1.2.2 was used to simulate a stylized 2-year pandemic-driven economic crisis, to examine what the transient climate response to an economic crisis (if any) would look like. This is not a study of the precise climate effects of COVID-19. For detection purposes, exaggerated changes to the emissions were

introduced. The RCP8.5 scenario was used as a baseline. Three sensitivity scenarios were created: emission reduction of carbon dioxide emissions (CO2 scenario), emission reduction of aerosols and aerosol precursors (AER scenario), and emission reduction of both (ALL scenario). Ten ensemble members were used in each scenario.

Substantial emission reduction of carbon dioxide, aerosols and aerosol precursors (ALL) resulted in immediate (2020–2022) and short-term (2020–2025) warming of global mean surface temperature (MST) compared to the baseline, by up to +0.06°C. A long-term cooler-than-baseline trend follows this until the end of the simulation at 2050, by up to −0.2°C. MSTs over the three regions of Asia, Europe, and North America had similar patterns. The long-term cooler-than-baseline MSTs were attributed to the effect of reduced atmospheric CO_2, since significant cooling in the simulation period as a whole occurred in the CO2 scenario. The short-term warmer-than-baseline MSTs were attributed to the effect of reduced atmospheric aerosols, since significant immediate warming occurred in the AER scenario.

In the AER scenario, atmospheric aerosols had returned to baseline levels by 2025, but global and regional MSTs remained significantly warmer than baseline for the period of 2020–2050 as a whole. Warmer-than-baseline MSTs persisted through the whole simulation period until 2050. This was especially so for European MST which was almost always warmer than baseline. This could be explained by inter-model differences in the phase of the North Atlantic Oscillation (NAO). The multi-decadal signal was likely due to the neutral phase of the NAO in the perturbed scenarios compared to the strongly negative phase in the baseline scenario. However, this explanation has difficulty explaining the warmer-than-baseline global and Asian MSTs.

Whether changes in emissions caused the differences in NAO phase is questionable. The differences we see may simply be due to internal variability, but the ensemble confidence intervals for the NAO index seem to differ between scenarios. The ensembles may be insufficiently large. Finally, a possibility is that forcing changes suppressed the strongly negative NAO phase of the baseline simulation.

This study was motivated by the concept of economic crises as "tropospheric reverse volcanic eruptions". Sudden emissions of air pollutants in the form of volcanic eruptions are known to trigger significant summer cooling (winter warming) over Europe (northern Europe), in both the year and following year of large tropical eruptions. The temperature anomaly is associated with a positive phase of the NAO (Fischer et al., 2007; Graf et al., 1994; Robock, 2000). The perturbations in question are clearly tropospheric and hence limited regionally, but recent findings suggest that aerosol forcing can drive multi-decadal signals (Qin et al., 2020).

An alternative concept is that of an "anthropogenic solar maximum", as a regional response to a net global change in albedo (Ineson et al., 2011; Shindell et al., 2003), although this would not be an exact analogy due to the spatially inhomogeneous distribution of pollutants, vertical differences in atmospheric heating, as well as the large portion of carbon dioxide emissions removed in the experiment. A third possibility is a slow response through oceanic pathways (Álvarez-García et al., 2008; Woollings et al., 2015). Due to the timescale of the response, some type of atmosphere-ocean interaction seems to be the most probable mechanism if forcing changes did impact the NAO state. Even so, one major unanswered question is why the negative NAO state was suppressed.

Nevertheless, this study shows that brief reductions in global anthropogenic driving can result in large transient regional climate response lasting about 5 years, possibly extending to decades. An unexpected result of this study is that reduction of carbon dioxide emissions for only 2 in 31 simulation years resulted in statistically significant cooler global MSTs for the whole period. However, the emission reductions were greatly exaggerated.

Studies more specific to the coronavirus pandemic of 2019 have examined specific climate responses. Yang et al. (2020) considered fast climate responses caused by abrupt reductions of aerosols in a model with prescribed sea surface temperatures and sea ice concentrations, finding surface warming over continental regions of the Northern Hemisphere in 2020. Gettelman et al. (2020) found that while the peak impact of the sharp drop in aerosol emissions on global surface temperature was very small (+0.03 K), the aerosol changes were the largest contribution to COVID-19 emissions induced temperature changes, dominating CO_2 effects in 2020. Forster et al. (2020) estimated that while the reduction in global sulfur dioxide emission

would cause short-term warming, the long-term effect of the pandemic-driven response would be negligible, with a cooling of around 0.01°C ± 0.005°C by 2030 compared to a baseline scenario that follows current national policies.

In this study, emissions of aerosols and concentrations of CO_2 were returned to their original trajectories after two years. In reality, the economic crisis may require an extended recovery. In a more complex scenario, different regions may react differently, and hence the patterns of aerosol emissions may change from prior to the crisis. The use of climate models for regional climate projections of the near-future (e.g., 2030, 2050, etc.) should be exercised with caution, since emissions depend on economic activity. Both epidemics and economic crises are expected to reoccur in long-term projections, but their stochastic nature means that they cannot be prescribed deterministically in emission scenarios. One frequently sees claims in popular media that pandemics will become more common in the future. If this were true, the potential climate effects of recurrent pandemic-induced socio-economic shocks should be studied.

Conflict of Interest

The authors declare no conflicts of interest relevant to this study.

Code Availability Statement

The code for the CESM 1.2 is publicly available at https://www.cesm.ucar.edu/models/cesm1.2/. The code for post-processing and figure creation is available on request from the corresponding author.

Data Availability Statement

The reanalysis data for assessing model results is available at https://climatedataguide.ucar.edu/climate-data/nasa-merra. Atmospheric CO_2 concentration under different RCP scenarios and the air pollutant emission inventory come from CESM1.2. The records of atmospheric CO_2 concentration from Global Monitoring Laboratory during 2000–2019 (Tans & Keeling 2021) is available at https://www.esrl.noaa.gov/gmd/ccgg/trends/data.html. Emissions input fields used to drive the simulations are downloaded automatically during the model building process. Model results shown in this paper are available online (http://doi.org/10.5281/zenodo.4112694).

Acknowledgments
This study was supported by National Key R&D Program of China (2016YFA0602703), and the Second Tibetan Plateau Scientific Expedition and Research Program (2019QZKK0103). The CESM project is supported primarily by the National Science Foundation. The authors thank all the scientists, software engineers, and administrators who contributed to the development of CESM 1.2. Besides, we thank Dongdong Yan for his help in programming.

References

Álvarez-García, F., Latif, M., & Biastoch, A. (2008). On multidecadal and quasi-decadal North Atlantic variability. *Journal of Climate*, *21*(14), 3433–3452. https://doi.org/10.1175/2007JCLI1800.1

Bethke, I., Outten, S., Otterå, O. H., Hawkins, E., Wagner, S., Sigl, M., & Thorne, P. (2017). Potential volcanic impacts on future climate variability. *Nature Climate Change*, *7*(11), 799–805. https://doi.org/10.1038/nclimate3394

Bittner, M., Schmidt, H., Timmreck, C., & Sienz, F. (2016). Using a large ensemble of simulations to assess the Northern Hemisphere stratospheric dynamical response to tropical volcanic eruptions and its uncertainty. *Geophysical Research Letters*, *43*, 9324–9332. https://doi.org/10.1002/2016GL070587

Bowen, G., Maibauer, B. J., Kraus, M. J., Röhl, U., Westerhold, T., Steimke, A., et al. (2015). Two massive, rapid releases of carbon during the onset of the Palaeocene–Eocene thermal maximum. *Nature Geoscience*, *8*, 44–47. https://doi.org/10.1038/ngeo2316

Bryan, K., Komro, F. G., Manabe, S., & Spelman, M. J. (1982). Transient climate response to increasing atmospheric carbon dioxide. *Science*, *215*(4528), 56–58. https://doi.org/10.1126/science.215.4528.56

Copernicus Atmosphere Monitoring Service (CAMS). (2020). *Amid Coronavirus outbreak: Copernicus monitors reduction of particulate matter (PM2.5) over China*. Retrieved from https://atmosphere.copernicus.eu/amid-coronavirus-outbreak-copernicus-monitors-reduction-particulate-matter-pm25-over-china

Duchon, C. E. (1979). Lanczos filtering in one and two dimensions. *Journal of Applied Meteorology*, *18*, 1016–1022. https://doi.org/10.1175/1520-0450(1979)018<1016:.LFIOAT>2.0.CO;2

European Space Agency. (2020a). *Air pollution remains low as Europeans stay at home*. Retrieved from https://www.esa.int/Applications/Observing_the_Earth/Copernicus/Sentinel-5P/Air_pollution_remains_low_as_Europeans_stay_at_home

European Space Agency. (2020b). *Air pollution drops in India following lockdown*. Retrieved from http://www.esa.int/Applications/Observing_the_Earth/Copernicus/Sentinel-5P/Air_pollution_drops_in_India_following_lockdown

European Space Agency. (2020c). *Coronavirus lockdown leading to drop in pollution across Europe*. Retrieved from https://www.esa.int/Applications/Observing_the_Earth/Copernicus/Sentinel-5P/Coronavirus_lockdown_leading_to_drop_in_pollution_across_Europe

European Space Agency. (2020d). *Coronavirus: Nitrogen dioxide emissions drop over Italy*. Retrieved from https://www.esa.int/ESA_Multimedia/Videos/2020/03/Coronavirus_nitrogen_dioxide_emissions_drop_over_Italy

European Space Agency. (2020e). *COVID-19: Nitrogen dioxide over China*. Retrieved from https://www.esa.int/Applications/Observing_the_Earth/Copernicus/Sentinel-5P/COVID-19_nitrogen_dioxide_over_China

Evans, S. (2020). Analysis: Coronavirus set to cause largest ever annual fall in CO_2 emissions. *Carbon Brief*. Retrieved from https://www.carbonbrief.org/analysis-coronavirus-set-to-cause-largest-ever-annual-fall-in-CO2-emissions

Eyring, V., Bony, S., Meehl, G. A., Senior, C. A., Stevens, B., Stouffer, R. J., & Taylor, K. E. (2016). Overview of the Coupled Model Intercomparison Project Phase 6 (CMIP6) experimental design and organization. *Geoscientific Model Development*, *9*, 1937–1958. https://doi.org/10.5194/gmd-9-1937-2016

Fischer, E. M., Luterbacher, J., Zorita, E., Tett, S. F. B., Casty, C., & Wanner, H. (2007). European climate response to tropical volcanic eruptions over the last half millennium. *Geophysical Research Letters*, *34*(5), 1–6. https://doi.org/10.1029/2006GL027992

Forster, P. M., Forster, H. I., Evans, M. J., Gidden, M. J., Jones, C. D., Keller, C. A., et al. (2020). Current and future global climate impacts resulting from COVID-19. *Nature Climate Change*, *10*, 913–919. https://doi.org/10.1038/s41558-020-0883-0

Gelaro, R., McCarty, W., Suárez, M. J., Todling, R., Molod, A., Takacs, L., et al. (2017). The modern-era retrospective analysis for research and applications, version 2 (MERRA-2). *Journal of Climate*, *30*(13), 5419–5454. https://doi.org/10.1175/JCLI-D-16-0758.1

Gettelman, A., Lamboll, R., Bardeen, C. G., Forster, P. M., & Watson-Parris, D. (2020). Climate impacts of COVID-19 induced emission changes. *Earth and Space Science Open Archive*, *13*. https://doi.org/10.1002/essoar.10505012.1

Gidden, M. J., Riahi, K., Smith, S. J., Fujimori, S., Luderer, G., Kriegler, E., et al. (2019). Global emissions pathways under different socioeconomic scenarios for use in CMIP6: A dataset of harmonized emissions trajectories through the end of the century. *Geoscientific Model Development*, *12*, 1443–1475. https://doi.org/10.5194/gmd-12-1443-2019

Graf, H. F., Perlwitz, J., & Kirchner, I. (1994). Northern Hemisphere tropospheric midlatitude circulation after violent volcanic eruptions. *Contributions to Atmospheric Physics*, *67*, 3–13.

Gregory, J., & Webb, M. (2008). Tropospheric adjustment induces a cloud component in CO_2 forcing. *Journal of Climate*, *21*(1), 58–71. https://doi.org/10.1175/2007JCLI1834.1

Held, I. M., Winton, M., Takahashi, K., Delworth, T., Zeng, F., & Vallis, G. K. (2010). Probing the fast and slow components of global warming by returning abruptly to preindustrial forcing. *Journal of Climate*, *23*(9), 2418–2427. https://doi.org/10.1175/2009JCLI3466.1

Hermanson, L., Bilbao, R., Dunstone, N., Ménégoz, M., Ortega, P., Pohlmann, H., et al. (2020). Robust multiyear climate impacts of volcanic eruptions in decadal prediction systems. *Journal of Geophysical Research: Atmospheres*, *125*(9), e2019JD031739. https://doi.org/10.1029/2019JD031739

Hurrell, J. W., Holland, M. M., Gent, P. R., Ghan, S., Kay, J. E., Kushner, P. J., et al. (2013). The community earth system model: A framework for collaborative research. *Bulletin of the American Meteorological Society*, *94*(9), 1339–1360. https://doi.org/10.1175/BAMS-D-12-00121.1

Ineson, S., Scaife, A. A., Knight, J. R., Manners, J. C., Dunstone, N. J., Gray, L. J., & Haigh, J. D. (2011). Solar forcing of winter climate variability in the Northern Hemisphere. *Nature Geoscience*, *4*, 753–757. https://doi.org/10.1038/ngeo1282

IPCC. (2013). In Stocker, T. F., Qin, D., Plattner, G.-K., Tignor, M., Allen, S. K., Boschung, J., et al. (Eds.), *Climate change 2013: The physical science basis. Contribution of working group I to the fifth assessment report of the intergovernmental panel on climate change* (p. 1535). Cambridge University Press.

IPCC. (2014). In Pachauri, R. K., & Meyer, L. A. (Eds.), *Climate change 2014: Synthesis report. Contribution of working groups I, II and III to the fifth assessment report of the intergovernmental panel on climate change [core writing team* (p. 151). IPCC.

Irvine, P., Emanuel, K., He, J., Horowitz, L. W., Vecchi, G., & Keith, D. (2019). Halving warming with idealized solar geoengineering moderates key climate hazards. *Nature Climate Change*, *9*, 295–299. https://doi.org/10.1038/s41558-019-0398-8

Kay, J. E., Deser, C., Phillips, A., Mai, A., Hannay, C., Strand, G., et al. (2015). The Community Earth System Model (CESM) large ensemble project: A community resource for studying climate change in the presence of internal climate variability. *Bulletin of the American Meteorological Society*, *96*(8), 1333–1349. https://doi.org/10.1175/BAMS-D-13-00255.1

Kenyon, J., & Hegerl, G. C. (2008). Influence of modes of climate variability on global temperature extremes. *Journal of Climate*, *21*(15), 3872–3889. https://doi.org/10.1175/2008JCLI2125.1

Le Quéré, C., Jackson, R. B., Jones, M. W., Smith, A. J. P., Abernethy, S., Andrew, R. M., et al. (2020). Temporary reduction in daily global CO_2 emissions during the COVID-19 forced confinement. *Nature Climate Change*, *10*, 647–653. https://doi.org/10.1038/s41558-020-0797-x

Li, C., Held, H., Hokamp, S., & Marotzke, J. (2020). Optimal temperature overshoot profile found by limiting global sea level rise as a lower-cost climate target. *Science Advances*, *6*, eaaw9490. https://doi.org/10.1126/sciadv.aaw9490

Li, J., & Wang, X. L. (2003). A new North Atlantic oscillation index and its variability. *Advances in Atmospheric Sciences*, *20*, 661–676. https://doi.org/10.1007/BF02915394

Liu, X., Easter, R. C., Ghan, S. J., Zaveri, R., Rasch, P., Shi, X., et al. (2012). Toward a minimal representation of aerosols in climate models: Description and evaluation in the Community Atmosphere Model CAM5. *Geoscientific Model Development*, *5*, 709–739. https://doi.org/10.5194/gmd-5-709-2012

Liu, Z., Ciais, P., Deng, Z., Lei, R., Davis, S. J., Feng, S., et al. (2020). *COVID-19 causes record decline in global CO_2 emissions*. arXiv preprints. Retrieved from https://arxiv.org/abs/2004.13614

Lohmann, U., Rotstayn, L., Storelvmo, T., Jones, A., Menon, S., Quaas, J., et al. (2010), Total aerosol effect: Radiative forcing or radiative flux perturbation? *Atmospheric Chemistry and Physics 10*, 3235–3246. https://doi.org/10.5194/acp-10-3235-2010

Moss, R. H., Edmonds, J. A., Hibbard, K. A., Manning, M. R., Rose, S. K., van Vuuren, D. P., et al. (2010). The next generation of scenarios for climate change research and assessment. *Nature*, *463*, 747–756. https://doi.org/10.1038/nature08823

Neale, R. B., Richter, J. H., Conley, A. J., Park, S., Lauritzen, P. H., Gettelman, A., & Williamson, D. L. (2010). *Description of the NCAR community atmosphere model (CAM 5.0)*. NCAR Technical Note NCAR/TN-486+ STR 1. 1, pp. 1–12.

Papale, D., Antoniella, G., Nicolini, G., Gioli, B., Zaldei, A., Vogt, R., et al. (2020). *Clear evidence of reduction in urban CO_2 emissions as a result of COVID-19 lockdown across Europe*. Integrated Carbon Observation System. Retrieved from https://www.icos-cp.eu/event/933

Persad, G. G., & Caldeira, K. (2018). Divergent global-scale temperature effects from identical aerosols emitted in different regions. *Nature Communications*, *9*(1), 3289. https://doi.org/10.1038/s41467-018-05838-6

Pinto, J. G., & Raible, C. C. (2012). Past and recent changes in the North Atlantic oscillation. *Wiley Interdisciplinary Reviews: Climate Change*, *3*, 79–90. https://doi.org/10.1002/wcc.150

Qin, M., Dai, A., & Hua, W. (2020). Aerosol-forced multidecadal variations across all ocean basins in models and observations since 1920. *Science Advances*, *6*(29), eabb0425. https://doi.org/10.1126/sciadv.abb0425

Raible, C. C., Brönnimann, S., Auchmann, R., Brohan, P., Frölicher, T. L., Graf, H. F., et al. (2016). Tambora 1815 as a test case for high impact volcanic eruptions: Earth system effects. *Wiley Interdisciplinary Reviews: Climate Change*, *7*, 569–589. https://doi.org/10.1002/wcc.407

Riahi, K., Grübler, A., & Nakicenovic, N. (2007). Scenarios of long-term socio-economic and environmental development under climate stabilization. *Technological Forecasting and Social Change*, *74*, 887–935. https://doi.org/10.1016/j.techfore.2006.05.026

Robock, A. (2000). Volcanic eruptions and climate. *Reviews of Geophysics*, *38*, 191–219. https://doi.org/10.1029/1998RG000054

Schmidt, H., Alterskjær, K., Bou Karam, D., Boucher, O., Jones, A., Kristjánsson, J. E., et al. (2012). Solar irradiance reduction to counteract radiative forcing from a quadrupling of CO_2: Climate responses simulated by four earth system models. *Earth Syst. Dyn.*, *3*(1), 63–78. https://doi.org/10.5194/esd-3-63-2012

Sharma, S., Zhang, M., Gao, J., Zhang, H., Kota, S. H., & Kota, S. H. (2020). Effect of restricted emissions during COVID-19 on air quality in India. *The Science of the Total Environment*, *728*, 138878. https://doi.org/10.1016/j.scitotenv.2020.138878

Sherwood, S. C., Bony, S., Boucher, O., Bretherton, C., Forster, P. M., Gregory, J. M., & Stevens, B. (2015). Adjustments in the forcing-feedback framework for understanding climate change. *Bulletin of the American Meteorological Society*, *96*(2), 217–228. https://doi.org/10.1175/BAMS-D-13-00167.1

Shindell, D. T., Schmidt, G. A., Miller, R. L., & Mann, M. E. (2003). Volcanic and solar forcing of climate change during the preindustrial era. *Journal of Climate*, *16*(24), 4094–4107. https://doi.org/10.1175/1520-0442(2003)016<4094:VASFOC>2.0.CO;2

Smith, D. M., Eade, R., Scaife, A. A., Caron, L.-P., Danabasoglu, G., DelSole, T. M., et al. (2019). Robust skill of decadal climate predictions. *npj Climate and Atmospheric Science*, *2*(1), 13. https://doi.org/10.1038/s41612-019-0071-y

Solomon, S., Daniel, J. S., Sanford, T. J., Murphy, D. M., Plattner, G.-K., Knutti, R., & Friedlingstein, P. (2010). Persistence of climate changes due to a range of greenhouse gases. *Proceedings of the National Academy of Sciences of the United States of America*, *107*(43), 18354–18359. https://doi.org/10.1073/pnas.1006282107

Swingedouw, D., Mignot, J., Ortega, P., Khodri, M., Menegoz, M., Cassou, C., & Hanquiez, V. (2017). Impact of explosive volcanic eruptions on the main climate variability modes. *Global and Planetary Change*, *150*, 24–45. https://doi.org/10.1016/j.gloplacha.2017.01.006

Tans, P., & Keeling, R. (2021). *Mauna Loa CO_2 annual mean data*. Retrieved from https://www.esrl.noaa.gov/gmd/ccgg/trends/data.html

Taylor, K. E., Stouffer, R. J., & Meehl, G. A. (2012). An overview of CMIP5 and the experiment design. *Bulletin of the American Meteorological Society*, *93*(4), 485–498. https://doi.org/10.1175/BAMS-D-11-00094.1

Textor, C., Schulz, M., Guibert, S., Kinne, S., Balkanski, Y., Bauer, S., et al. (2005). Analysis and quantification of the diversities of aerosol life cycles within AeroCom. *Atmospheric Chemistry and Physics*, *6*, 1777–1813. https://doi.org/10.5194/acp-6-1777-2006

Volcovici, V. (2020). *Urban air quality improves as coronavirus empties U.S. Highways: NOAA*. Reuters. Retrieved from https://www.reuters.com/article/us-health-coronavirus-usa-pollution/urban-air-quality-improves-as-coronavirus-empties-us-highways-noaa-idUSKBN22P1OV

Wang, H., Xie, S., & Liu, Q. (2016). Comparison of climate response to anthropogenic aerosol versus greenhouse gas forcing: Distinct patterns. *Journal of Climate*, *29*(14), 5175–5188. https://doi.org/10.1175/JCLI-D-16-0106.1

Woollings, T., Franzke, C., Hodson, D. L. R., Dong, B., Barnes, E. A., Raible, C. C., & Pinto, J. G. (2015). Contrasting interannual and multidecadal NAO variability. *Climate Dynamics*, *45*, 539–556. https://doi.org/10.1007/s00382-014-2237-y

Yang, Y., Ren, L., Li, H., Wang, H., Wang, P., Chen, L., et al. (2020). Fast climate responses to aerosol emission reductions during the COVID-19 pandemic. *Geophysical Research Letters*, *47*, e2020GL089788. https://doi.org/10.1029/2020GL089788